


Article

Activation of Endoplasmic Reticulum-Localized Metabotropic Glutamate Receptor 5 (mGlu₅) Triggers Calcium Release Distinct from Cell Surface Counterparts in Striatal Neurons

Yuh-Jiin I. Jong, Steven K. Harmon and Karen L. O'Malley * 

Department of Neuroscience, Washington University School of Medicine, Saint Louis, MO 63110, USA; jongi@wustl.edu (Y.-J.I.J.); harmons@wustl.edu (S.K.H.)

* Correspondence: omalleyk@wustl.edu; Tel.: +1-314-362-7087; Fax: +1-314-362-3446

Abstract: Metabotropic glutamate receptor 5 (mGlu₅) plays a fundamental role in synaptic plasticity, potentially serving as a therapeutic target for various neurodevelopmental and psychiatric disorders. Previously, we have shown that mGlu₅ can also signal from intracellular membranes in the cortex, hippocampus, and striatum. Using cytoplasmic Ca²⁺ indicators, we showed that activated cell surface mGlu₅ induced a transient Ca²⁺ increase, whereas the activation of intracellular mGlu₅ mediated a sustained Ca²⁺ elevation in striatal neurons. Here, we used the newly designed ER-targeted Ca²⁺ sensor, ER-GCaMP6-150, as a robust, specific approach to directly monitor mGlu₅-mediated changes in ER Ca²⁺ itself. Using this sensor, we found that the activation of cell surface mGlu₅ led to small declines in ER Ca²⁺, whereas the activation of ER-localized mGlu₅ resulted in rapid, more pronounced changes. The latter could be blocked by the Gq inhibitor FR9000359, the PLC inhibitor U73122, as well as IP₃ and ryanodine receptor blockers. These data demonstrate that like cell surface and nuclear mGlu₅, ER-localized receptors play a pivotal role in generating and shaping intracellular Ca²⁺ signals.

Keywords: metabotropic glutamate receptor 5 (mGlu₅); endoplasmic reticulum (ER); calcium; G protein-coupled receptor (GPCR); N-methyl-D-aspartic acid (NMDA)



Academic Editor: Guangyu Wu

Received: 27 January 2025

Revised: 12 March 2025

Accepted: 4 April 2025

Published: 9 April 2025

Citation: Jong, Y.-J.I.; Harmon, S.K.; O'Malley, K.L. Activation of Endoplasmic Reticulum-Localized Metabotropic Glutamate Receptor 5 (mGlu₅) Triggers Calcium Release Distinct from Cell Surface Counterparts in Striatal Neurons. *Biomolecules* **2025**, *15*, 552. <https://doi.org/10.3390/biom15040552>

Copyright: © 2025 by the authors. Licensee MDPI, Basel, Switzerland. This article is an open access article distributed under the terms and conditions of the Creative Commons Attribution (CC BY) license (<https://creativecommons.org/licenses/by/4.0/>).

1. Introduction

As a universal signaling molecule, calcium (Ca²⁺) is a critical intracellular second messenger [1–3]. Cytosolic Ca²⁺ signals are generated via Ca²⁺ release from intracellular stores like the endoplasmic reticulum (ER) or via entry from the extracellular space. In the former, activation of cell surface receptors such as G protein-coupled receptors (GPCRs) or receptor tyrosine kinases (RTKs) can lead to the activation of phospholipase C (PLC), the cleavage of phosphatidyl inositol 4, 5 biphosphate (PIP₂) and the production of inositol 1,4,5 trisphosphate (IP₃) [4]. IP₃ binding to IP₃ receptors on the ER membrane allows Ca²⁺ to be released from luminal stores, affecting many cytoplasmic signaling systems. Ca²⁺ within the ER lumen also plays a signaling role [5–7], affecting the ability of the ER to communicate with other organelles as well as supporting critical ER functions such as protein folding and lipid biosynthesis. Not surprisingly, disruption of ER Ca²⁺ homeostasis can lead to ER stress, loss of mitochondrial function, apoptosis, and cell death [8]. Thus, transient increases of cytoplasmic Ca²⁺ as well as perturbation of luminal Ca²⁺ can both lead to a variety of cell biological phenomena critical to cellular homeostasis.

Metabotropic glutamate receptors (mGlu receptors) are a family of GPCRs that modulate neuronal excitability and synaptic transmission in the central nervous system [9,10]. In

particular, the mGlu subtype, mGlu₅, plays a fundamental role in synaptic plasticity primarily by regulating intracellular Ca²⁺ levels via release from ER Ca²⁺ stores. Many studies have shown that activated plasma membrane mGlu₅ couples to G_{q/11} and phosphatidylinositol (PI)-PLC to generate IP₃-mediated release of Ca²⁺ from both IP₃ and ryanodine intracellular receptors. Depending upon the cell type in which the receptor is expressed, activation of cell surface mGlu₅ can generate a rapid, transient Ca²⁺ signal or a slowly decaying oscillatory response [11–13].

Over the last two decades, work from this lab has also shown that mGlu₅ is one out of a growing number of GPCRs [14–16] that can signal from intracellular membranes [17–22]. Specifically, more than 90% of mGlu₅ is present on intracellular membranes such as the ER and the nuclear membrane, where it can be activated by ligands that can be transported across cell membranes [17]. Like mGlu₅ present on the cell surface, activation of endogenous mGlu₅ receptors expressed on the inner membrane of isolated striatal nuclei also generate IP₃, leading to the IP₃-mediated release of Ca²⁺ in the nucleus [17,23]. Interestingly, in the striatum, mGlu₅-activated nuclear response patterns yield long prolonged Ca²⁺ responses (>10 min; 17). These data showed that the nucleus could function as an autonomous organelle independent of signals originating in the cytoplasm, and that nuclear mGlu₅ receptors play a dynamic role in mobilizing Ca²⁺ in a specific, localized fashion.

To directly monitor mGlu₅-mediated changes in ER Ca²⁺ itself, we used the newly designed and optimized ER-targeted Ca²⁺ sensor, ER-GCaMP6-150 [24], as a robust, specific approach to bypass less interpretable changes in cytosolic Ca²⁺ versus changes in ER Ca²⁺ content. Using this tool, we found that activation of cell surface mGlu₅ using DHPG led to a modest decline in somal ER Ca²⁺, whereas activation of intracellular mGlu₅ using Quis resulted in more pronounced soma ER Ca²⁺ changes. In either case, the effects were almost two-fold larger when measured in neurites. ER-localized mGlu₅-mediated Ca²⁺ responses could also be blocked by the Gq inhibitor, FR9000359, and the PLC inhibitor, U73122, but not by U73343. Finally, both IP₃ and ryanodine receptor blockers prevented ER mGlu₅-mediated decreases in luminal Ca²⁺. Collectively, these studies show that like cell surface and nuclear receptors, activated ER mGlu₅ receptors couple to G_{q/11} and PLC to generate the IP₃-mediated release of Ca²⁺ from Ca²⁺-release channels in the ER. Thus, the ER can also function as an autonomous organelle in mobilizing Ca²⁺ in a specific, localized fashion.

2. Materials and Methods

2.1. Materials

(+)- α -Amino-3,5-dioxo-1,2,4-oxadiazolidine-2-propanoic acid, quisqualate (Quis), (S)-3,5-dihydroxyphenylglycine (DHPG), 2-methyl-6-(phenylethynyl)pyridine (MPEP), 7-(hydroxyimino)-cyclopropan[b]chromen-1a-carboxylate ethyl ester (CPCCOEt), (\pm)-4-(4-aminophenyl)-1,2-dihydro-1-methyl-2-propylcarbamoyl-6,7-methylenedioxyphthalazine (SYM2206), 2-Aminoethoxydiphenylborane (2-APB), 1-[6-[(17 β)-3-Methoxyestra-1,3,5(10)-trien-17-yl]amino]hexyl]-1H-pyrrole-2,5-dione (U73122), and 1-[6-[(17 β)-3-Methoxyestra-1,3,5(10)-trien-17-yl]amino]hexyl]-2,5-pyrrolidinedione (U73343) were purchased from Tocris (Bio-Techne Corporation, Minneapolis, MN, USA). (4R,6S,8S,10Z,12R,14R,16E,18R,19R,20S,21S)-11,19,21-trihydroxy-4,6,8,12,14,18,20-heptamethyl-22-[(2S,2'R,5S,5'S)-octahydro-5'-[(1R)-1-hydroxyethyl]-2,5'-dimethyl [2,2'-bifuran]-5-yl]-9-oxo-10,16-docosadienoic acid (Ionomycin) and 1-[[[5-(4-nitrophenyl)-2-furanyl]methylene]amino]-2,4-imidazolidinedione, monosodium salt (Dantrolene) were purchased from Cayman Chemical (Ann Arbor, MI, USA). N-methyl-D-aspartic acid (NMDA) was purchased from Sigma-Aldrich (St. Louis, MO, USA). 2-Amino-2-(3-cis/trans-carboxycyclobutyl)-3-(9H-thioxanthen-9-yl) propionic acid (LY393053) was obtained from Lilly Research Laboratories, Eli Lilly and Company

(Indianapolis, IN, USA). (3R)-N-acetyl-3-hydroxy-L-leucyl-(α R)- α -hydroxybenzenepropanoyl-2,3-didehydro-N-methylalanyl-L-alanyl-N-methyl-L-alanyl-(3R)-3-[[[(2S,3R)-3-hydroxy-4-methyl-1-oxo-2-[(1-oxopropyl)amino]pentyl]oxy]-L-leucyl-N,O-dimethyl-L-threonine, (7 \rightarrow 1)-lactone (FR900359) [25] was a gift from Dr. Ken Blumer (Washington University School of Medicine, St. Louis, MO, USA).

2.2. Plasmid Constructs

ER-GCaMP6-150 (Addgene plasmid #86918; 24) was a gift from Dr. Ghazaleh Ashrafi (Washington University School of Medicine) with permission from Dr. Timothy Ryan (Weill Cornell Medicine, New York, NY, USA).

2.3. Primary Neuronal Culture and Transfection

Primary striatal cultures using neonatal 1-day-old rat pups were prepared and maintained as previously described [17,26]. The cells were plated onto poly-d-lysine-coated, glass-inserted P35 dishes (14 mm; 60,000/glass, Cellvis, Mountain View, CA, USA) for immunostaining or Ca^{2+} real-time imaging. Cells were cultured in humidified air with 5% CO_2 at 37 °C. The cultures were transfected with ER-GCaMP6-150 at DIV (days in vitro) 11 using Lipofectamine 2000 (Thermo Fisher Scientific, Waltham, MA, USA) and immunostained or imaged in real time 4–7 days after transfection as previously described [18].

2.4. Immunocytochemistry

After transfection, primary striatal cultures at DIV 15–18 were fixed and stained as described previously [18]. Primary antibodies included mouse monoclonal anti-calnexin (1:50; BD Bioscience, Becton, NJ, USA) and chicken polyclonal anti-GFP (1:2000; Aves Labs., Tigard, OR, USA). Secondary antibodies included goat anti-mouse Cy3 (1:300; Jackson ImmunoResearch, West Grove, PA, USA) and goat anti-chicken Alexa 488 (1:500; Molecular Probes, Eugene, OR, USA).

2.5. Measurement of ER Ca^{2+} Dynamics

ER-targeted, low-affinity GCaMP6-150 was used to measure ER Ca^{2+} dynamics. Transfected striatal neurons were preincubated with control medium (125 mM NaCl, 5 mM KCl, 20 mM Hepes, 1.5 mM CaCl_2 , 1.5 mM MgCl_2 , 10 mM glucose, pH 7.4) containing mGlu₁ antagonist, CPCCOEt (20 μM), and AMPA receptor, antagonist SYM2206 (25 μM), for 30 min at 37 °C before adding DHPG (100 μM) to measure cell surface mGlu₅ activation. In addition, the impermeable, non-transported mGlu₅ antagonist, LY393053 (LY53, 20 μM) [17], was included in the incubation buffer before adding Quis (20 μM) to measure specific intracellular mGlu₅ activation. To study the pathways involved in intracellular mGlu₅ activation, U-73122 (phospholipase C inhibitor, 10 μM), U73343 (inactive analog of U73122, 10 μM), 2-APB (IP3 receptor inhibitor, 100 μM), Dantrolene (ryanodine receptor inhibitor, 10 μM), or FR900359 ($\text{G}_{q/11}$ inhibitor, 1 μM) was also included in the incubation buffer before adding Quis. In all cases, drugs at 100x concentrations were added to the side of the dish by hand-held pipette and allowed to diffuse over the cells.

2.6. Confocal Microscopy and Data Analysis

Fluorescent Measurements of ER Ca^{2+} were performed and quantitated as described previously [22]. Briefly, 4–7 days after transfection with GCaMP6-150, ER Ca^{2+} imaging in striatal neurons was conducted using a laser confocal microscope (Olympus BX 50WI, Center Valley, PA, USA) Fluoview1200 with an Olympus LUMPlanFI/IR 40 \times /0.80w objectives. Cultures were preincubated with a control medium and treated as described above. The real-time ER Ca^{2+} images were conducted at 3–5 sec intervals and collected by an Olympus Fluoview FVX Confocal Laser Scanning system using Fluoview 4.2 ac-

quisition software ([https://www.olympus-lifescience.com/en/downloads/detail-iframe/?0\[downloads\]\[id\]=847249651](https://www.olympus-lifescience.com/en/downloads/detail-iframe/?0[downloads][id]=847249651)) (accessed on 11 February 2021). Images were processed with MetaMorph (version 7.7) (<https://www.moleculardevices.com/products/cellular-imaging-systems/acquisition-and-analysis-software/metamorph-microscopy>) (accessed on 14 April 2023) Professional Image Analysis software, produced by Universal imaging corporation (Downingtown, PA, USA). Immunofluorescence was analyzed around the soma area or in proximal dendrites at a distance of 40 μm . The average intensity across all images in soma and neurites was calculated at each time point for each category treated with different agonists or antagonists and then compared. Fluorescent ER Ca^{2+} signals, in response to electrical activity (ΔF), were normalized to the resting fluorescence (F_0). The F_0 value was additionally corrected for background autofluorescence measured in a nearby non-transfected region. Separate controls were performed with each experiment, and Student's *t* test was used to determine statistical significance. Half maximal response times ($T_{1/2}$) were assessed from the slopes of drug-induced ER Ca^{2+} loss curves derived from the first significant point of deflection outwards to 100 s. The statistical analysis was performed by GraphPad prism 10.2 (GraphPad software, Boston, MA, USA). Aggregated data ($N = 12$ for each condition) were analyzed via one-way of variance (ANOVA) followed by Tukey's multiple comparison test.

2.7. Animal Studies

All animal procedures were performed according to NIH guidelines and approved by the Washington University Institutional Animal Care and Use Committee under protocols 21-0052 and 22-0228. Animals were under the care of the Washington University School of Medicine Division of Comparative Medicine.

3. Results

ER-GCaMP6-150 as an ER Ca^{2+} indicator: Previously, we demonstrated that ER-localized mGlu₅ receptors would be oriented such that the ligand-binding domain is within the ER lumen. As such, agonists must cross both the cell surface lipid bilayer as well as the ER membrane for receptor activation [17,18,23]. Mechanistically, agonist transport is achieved via the sodium-dependent glutamate transporter and/or the cystine, glutamate xCT exchanger [17,18]. Using radiolabeled glutamate and Quis, as well as uptake studies and knock-out animals, we showed that the mGlu₅ agonist DHPG is a non-transported, non-permeable agonist, whereas glutamate and Quis enter the cell via active transport [17]. Although we see similar results in cortex, hippocampus, and spinal cord dorsal horn neurons [17–20], we typically use primary dissociated striatal neurons because >70% of the neurons are medium spiny neurons that express mGlu₅ [17]. Inasmuch as the G protein binding portion of mGlu₅ is in the cytoplasm, after ligand binding, $G_{q/11}$ -coupled receptors like mGlu₅ activate PLC which, in turn, hydrolyzes the membrane PIP_2 into the second messengers IP_3 and diacylglycerol (DAG). IP_3 can then activate IP_3 receptors on the ER membrane, leading to the release of ER Ca^{2+} . A schematic representation of these interactions is shown in Figure 1. The release of ER Ca^{2+} is frequently measured as an increase in cytoplasmic Ca^{2+} assessed by the Ca^{2+} indicator dye, Oregon GreenTM 488 BAPTA-1, AM. Alternatively, and more directly, decreases in ER Ca^{2+} content can be directly monitored by the loss of luminal fluorescence using the genetically encoded Ca^{2+} sensor, ER-GCaMP6-150 [24], that is restricted to the ER throughout the neuron (Figure 2A) and co-localizes with the ER marker calnexin (Figure 2B). Real-time imaging of somatic ER-GCaMP6-150 before and after the addition of either DMSO as a treatment control or the Ca^{2+} ionophore, ionomycin, are shown in Figure 2C and quantified in Figure 2D. Consistent

with published reports using this sensor [24], ionomycin (4 μ M) treatment led to a rapid decrease in ER Ca^{2+} levels (Figure 2C,D).

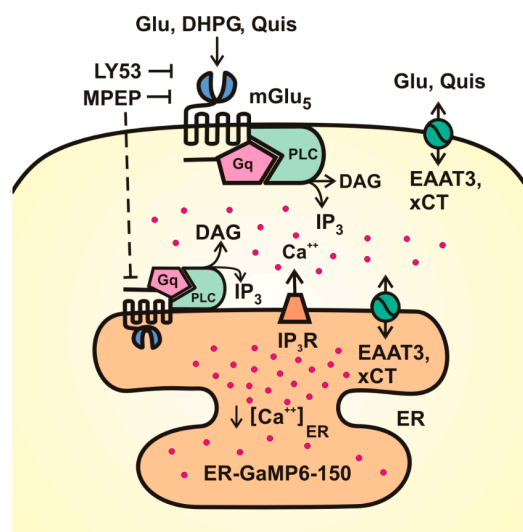


Figure 1. Schematic representation of cell surface and ER-localized mGlu₅ receptor signaling in striatal neurons. Glu (glutamate) and Quis (quisqualate) act as impermeable, transported agonists and thus activate both the cell surface and intracellular mGlu₅ receptor. DHPG is an impermeable, non-transported mGlu₅ agonist; accordingly, it activates only cell surface receptors. LY53 (LY393053) is an impermeable, non-transported antagonist whereas MPEP is a permeable mGlu₅ antagonist. Effectors downstream include Gq, phospholipase C (PLC), diacylglycerol (DAG), and IP₃. The latter acts at IP₃ receptors (IP₃R) to release luminal ER Ca^{2+} . This can be measured in real time via ER-GaMP6-150. EAAT3 (excitatory amino acid transporter 3) or xCT (cystine/glutamate exchanger) are bidirectional Glu or Quis transporters.

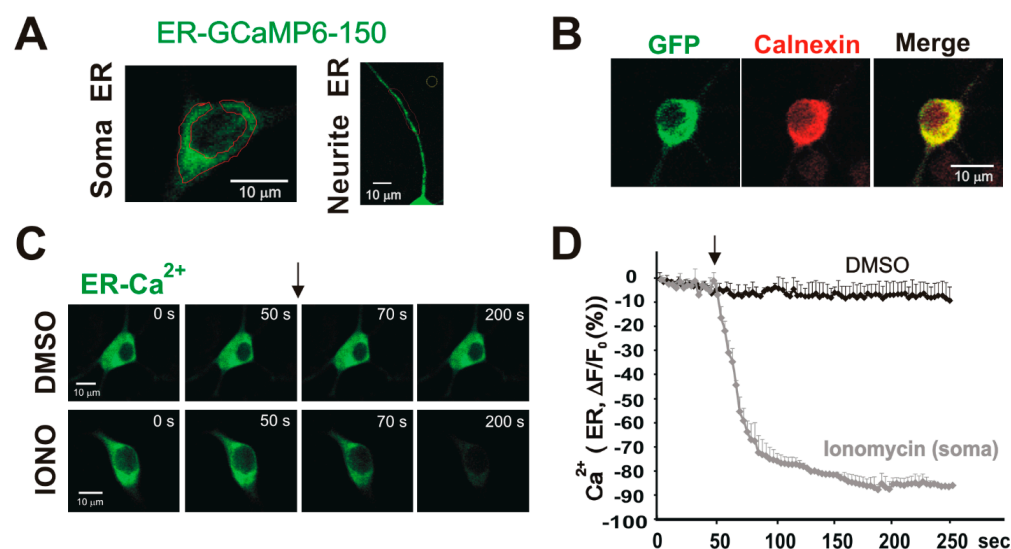


Figure 2. ER-GCaMP6-150 is an ER Ca^{2+} indicator. Ionomycin triggers rapid ER Ca^{2+} release in soma and neurites of striatal neurons. Striatal neurons transfected with ER-GCaMP6-150 at DIV 11 were immunostained or imaged by laser confocal microscope (Olympus BX 50WI) Fluoview1200 at DIV 15–18. (A) High-resolution image of striatal neurons transfected with ER-GCaMP6-150 showing ER structure in soma (left) and neurites (right). (B) The GCaMP6 expression is co-localized with the ER marker calnexin. (C) Time-lapse montages of striatal neurons transfected with ER Ca^{2+} probe (ER-GCaMP6-150) and treated with DMSO (0.04%) or ionomycin (4 μ M). (D) Graphic quantifying changes in ER Ca^{2+} upon treatment with DMSO or ionomycin. Ionomycin induced a rapid decrease in ER Ca^{2+} (DMSO or 4 μ M ionomycin was applied at the time indicated by the arrow, $n = 12$ for each condition).

mGlu₅ agonists trigger ER Ca²⁺ release in soma and neurites of striatal neurons: Once the correct targeting of ER-GCaMP6-150 to the ER was verified, endogenous mGlu₅ receptor-mediated Ca²⁺ responses were determined using pharmacological isolation of either cell surface or ER-localized receptors as we have described [18]. Consistent with the previous data, bath application of the transported agonist, Quis, generated a pronounced loss of ER Ca²⁺ in both neuronal cell bodies (-29.46 ± 4.59 S.E.M, $n = 3$) and neurites (-47.92 ± 4.88 S.E.M, $n = 3$) 100 sec after treatment (Figure 3A–C). These changes were entirely due to activation of ER-restricted mGlu₅ since they occurred in the presence of the impermeable, non-transported antagonist, LY393053, which we have shown to block all cell surface mGlu₅ receptor contributions [18] (Figure 3A–C). In contrast, pretreatment with the cell-permeant, mGlu₅ antagonist, MPEP, blocked all Quis responses (Figure 3C,E). To directly assess cell surface mGlu₅'s ability to release ER Ca²⁺, sibling cultures transfected with ER-GCaMP5-150, were treated with the impermeable, non-transported agonist, DHPG. DHPG led to an ER Ca²⁺ loss of $18.85\% \pm 2.13$ S.E.M, $n = 3$ in the soma and a loss of $25.35\% \pm 5.37$ S.E.M, $n = 3$ in the neurites. Notably, DHPG had a more modest effect in triggering ER Ca²⁺ release than Quis (~66% of a Quis somal response and 55% of a Quis neurite response; Figure 3D,E). In comparison to ionomycin, which, at 100 sec, has maximally released ER Ca²⁺ levels from the soma (Figure 2D; $-78.50\% \pm 0.24$ S.E.M, $n = 3$) or neurites ($-83.79\% \pm 7.6$ S.E.M, $n = 3$). At that same time point, DHPG released only 25–30% of ER Ca²⁺ measured in striatal soma or neurites, respectively. Quis activation of ER-localized mGlu₅ receptors led to the release of ~40% of somal ER Ca²⁺ in comparison to ionomycin, but >50% of maximal ER Ca²⁺ release in striatal neurites (Figure 3E). Taken together, these data unequivocally establish that ER-localized mGlu₅ is functionally active and is the major contributor to the increased cytoplasmic Ca²⁺ levels following receptor activation.

Quis triggers more rapid ER Ca²⁺ release than DHPG in striatal neurons: Using this same preparation of dissociated striatal neurons, we previously showed that cell surface-localized and intracellular mGlu₅ are associated with distinct patterns of Ca²⁺ release such that cell surface receptors exhibited rapid transient Ca²⁺ responses, whereas intracellular mGlu₅ exhibited sustained Ca²⁺ signals [18,21]. Examining the slopes of ER Ca²⁺ release over time following Quis or DHPG treatment in Figure 3C,D, it is clear that Ca²⁺ is being released more rapidly following Quis application in the soma and the neurites than is the case following DHPG addition. To quantify these differences, we calculated the T_{1/2} after drug application based on experimental curves such as those represented in Figures 2D and 3C,D. In keeping with the data shown in Figures 2 and 3, Quis triggered a more rapid ER Ca²⁺ release than DHPG at 100 sec in striatal cell bodies ($29.86 \text{ s} \pm 4.18 \text{ SD}$) and especially neurites ($20.33 \text{ s} \pm 6.23 \text{ SD}$; Figure 4). Ionomycin was $13.95 \text{ s} \pm 4.37 \text{ SD}$ in cell bodies and $6.40 \text{ s} \pm 2.32 \text{ SD}$ in neurites. DHPG exhibited a T_{1/2} of $43.06 \text{ s} \pm 8.02 \text{ SD}$ in cell bodies and $39.83 \text{ s} \pm 9.83 \text{ SD}$ in neurites. In striatal neurites, Quis was ~60% of the ionomycin rate of ER Ca²⁺ release, whereas DHPG was only 30% (Figure 4). Even at 5 s, Quis was >50% of the ionomycin release rate, while DHPG was not significantly different than the DMSO control (Figures 2D and 3D). Collectively, these data indicate that the activation of the ER-localized mGlu₅ receptor releases more total ER Ca²⁺ at a faster rate than the activation of cell surface receptors.

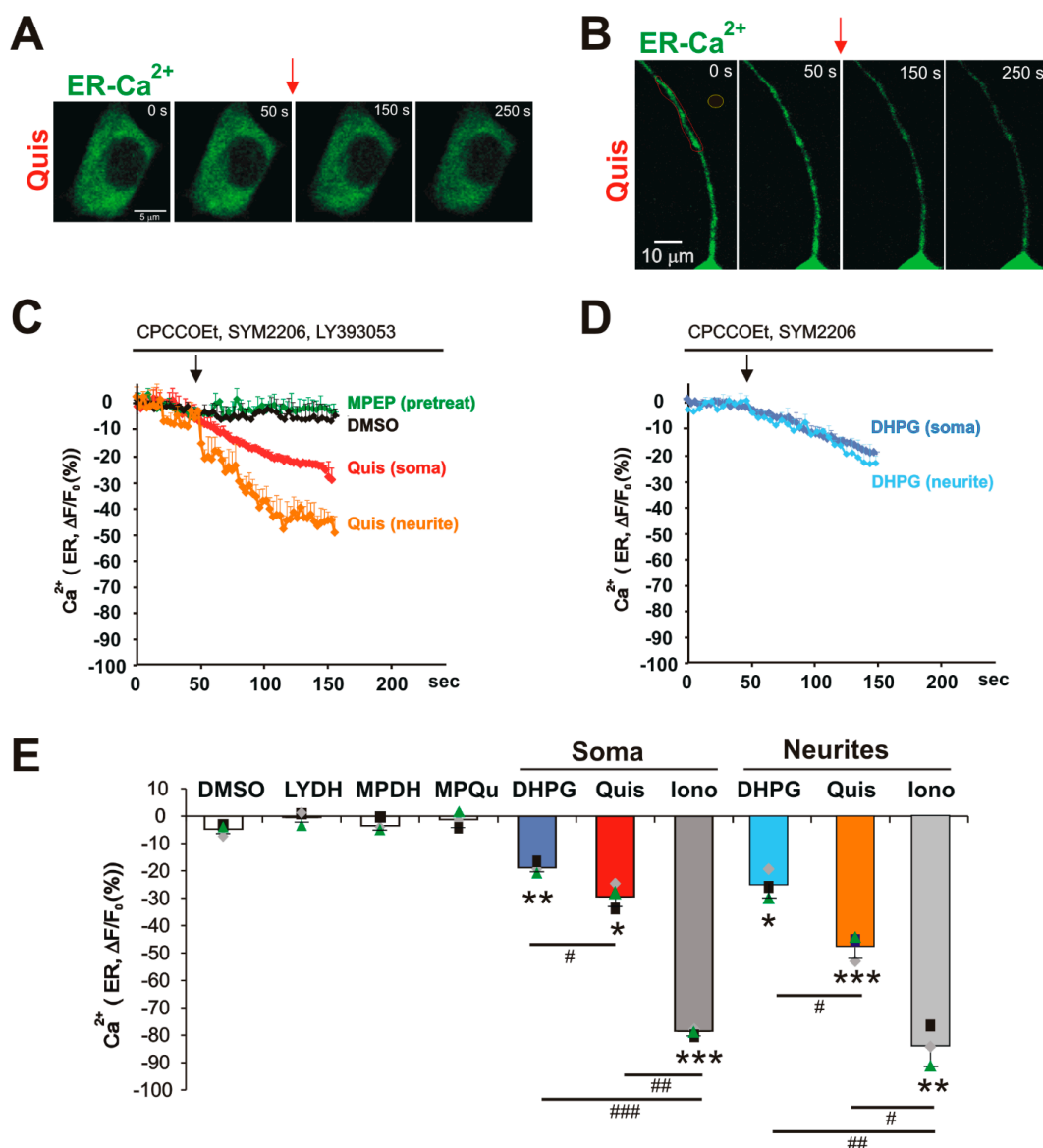


Figure 3. mGlu₅ agonists trigger ER Ca²⁺ release in soma and neurites of striatal neurons. Striatal neurons transfected with ER-GCaMP6-150 and imaged as described in methods. (A,B) Time-lapse montages of soma (A) or neurites (B) of striatal neurons transfected with ER Ca²⁺ probe (ER-GCaMP6-150) and treated with Quis (20 μM). (C,D) Graphic quantifying changes in ER Ca²⁺ upon treatment with Quis (20 μM) or DHPG (100 μM). Quis or DHPG was applied at the time indicated by the arrow. (C) Quis triggered a pronounced ER Ca²⁺ release in soma and neurites of striatal neurons, whereas (D) DHPG triggered a more modest ER Ca²⁺ release. (E) Changes in ER Ca²⁺ 100 s after treatment with various drugs. LYDH represents LY393053 pretreatment prior to DHPG addition; MPDH refers to MPEP pretreatment prior to DHPG or Quis (MPQu). Bars represent the mean of three experiments, ±S.E.M, from 12 neurons in each condition. Individual experiments are denoted by a ▲, ■, or ◆. *, ** denotes statistical significance compared to DMSO treatment with a Student's t test: * *p* < 0.05, ** *p* < 0.01, *** *p* < 0.001 (soma ER: *p* = 0.005 for DHPG, *p* = 0.012 for Quis, *p* = 0.0002 for ionomycin; neurite ER: *p* = 0.02 for DHPG, *p* = 0.0007 for Quis, *p* = 0.002 for ionomycin). # denotes statistical significance compared increased levels with different treatment using a Student's t test: # *p* < 0.05, ## *p* < 0.01, ### *p* < 0.001 (soma ER: *p* = 0.046 for DHPG versus Quis, *p* = 0.0002 for DHPG versus ionomycin, *p* = 0.0014 for Quis versus ionomycin; neurite ER: *p* = 0.031 for DHPG versus Quis, *p* = 0.003 for DHPG versus ionomycin, *p* = 0.012 for Quis versus ionomycin).

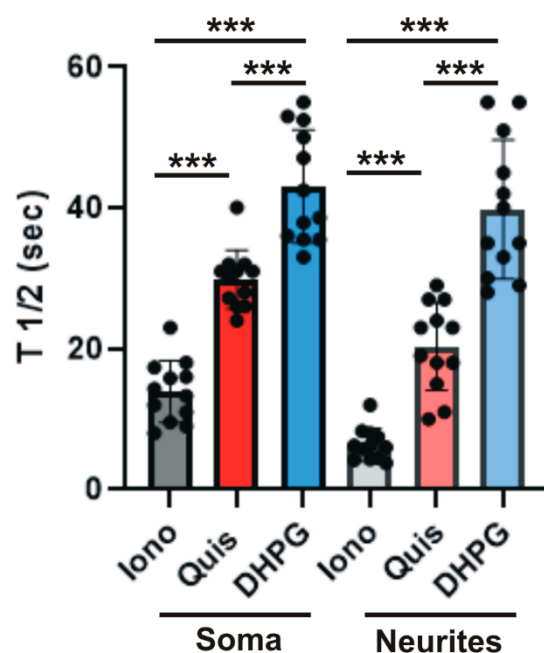
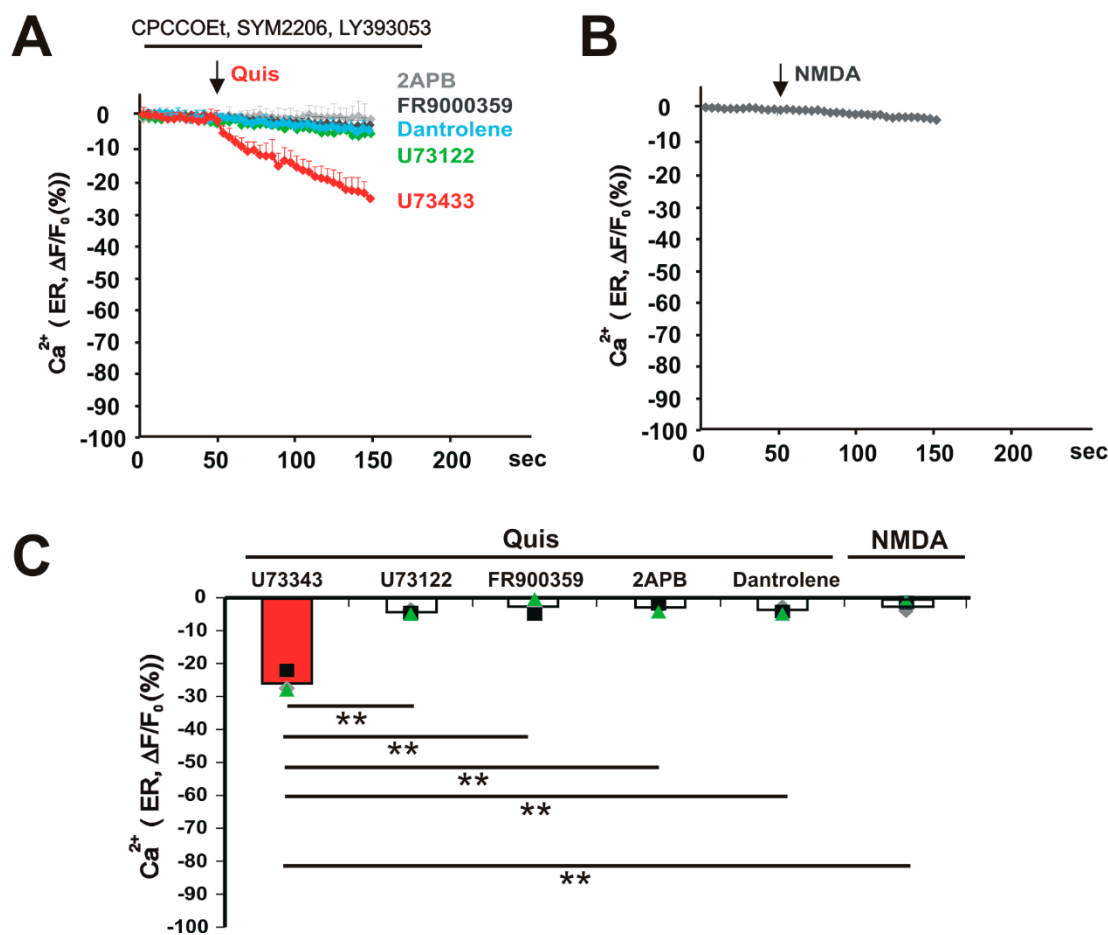


Figure 4. Quis triggers a more rapid ER Ca^{2+} release than DHPG in striatal neurons. Bar graphs of ER Ca^{2+} release $T_{1/2}$ at 100 s after drug application based on the curves in Figures 2D and 3C,D. Each point represents one cell ($N = 12$ for each condition, error bars represent standard deviation). *** $p < 0.001$, *** denotes statistical significance between different groups. Black dots represent individual neurons. The groups were compared by one-way ANOVA followed by Tukey test.

ER Ca^{2+} release triggered by Quis is blocked by U-73122, FR900359, 2-APB, and Dantrolene: ER-resident GPCRs appear to use a variety of G proteins to activate downstream pathways. In particular, release of ER Ca^{2+} has been linked to pertussis toxin-sensitive pathways, suggesting $G_{i/o}$ -driven mechanisms [27]. However, we have previously shown that, in HEK293 cells stably expressing mGlu₅ and/or endogenous receptors expressed in striatal neurons, pertussis toxin does not affect mGlu₅-mediated Ca^{2+} changes [23,28]. Rather, in either case, mGlu₅ couples with $G_{q/11}$ /PLC/IP₃ to release cytoplasmic and nucleoplasmic Ca^{2+} . Similarly, we hypothesized that ER-localized mGlu₅ couples to $G_{q/11}$ proteins to activate downstream signaling components. To confirm whether activated ER-localized mGlu₅ coupled to PLC to generate IP₃-mediated release of Ca^{2+} , we used the same real-time imaging assay of somatic ER-GCaMP6-150 before and after the addition of Quis in striatal neurons preincubated with various inhibitors such as 1 μM FR900359 ($G_{q/11}$ inhibitor), 10 μM U73122 (a PLC inhibitor), 10 μM U73343 (an inactive analog of U73122), 100 μM 2-APB (an IP₃ receptor inhibitor), and 10 μM Dantrolene (ryanodine receptor inhibitor). Results showed that ER Ca^{2+} release triggered by Quis was blocked by FR900359 (-2.74 ± 1.59 S.E.M), U-73122 (-4.37 ± 0.48 S.E.M), 2-APB (-2.94 ± 0.87 S.E.M), and Dantrolene (-3.72 ± 0.75 S.E.M). It was not blocked by U73343 (-25.85 ± 2.34 S.E.M; Figure 5A,C). These data confirm that, just like cell surface and nuclear receptors, ER-localized mGlu₅ also couples to $G_{q/11}$ to activate cytoplasmic PI-PLC, leading to the hydrolysis of PIP₂ and generation of IP₃. The latter leads to the release of Ca^{2+} from the ER into the cytoplasm. Collectively, these data show that ER-localized mGlu₅ can function independently of signals originating at the cell surface and thus plays a dynamic role in mobilizing Ca^{2+} in a specific, localized manner.



4. Discussion

A growing body of data has established that GPCRs not only signal from the cell surface but also from intracellular compartments. One such receptor is mGlu₅ which, over 20 years ago, was shown to be present and active not only on the cell surface but also on isolated nuclei [28]. Since mGlu₅ couples to G_{q/11}, these experiments used Ca²⁺ indicators such as Oregon Green BAPTA-AM or Fura2 to measure real-time changes in cytosolic Ca²⁺ levels as a proxy for release of ER Ca²⁺ [17,21]. Data from those experiments indicated that functional activity is generated by at least two separate pools of mGlu₅—on the cell surface and on the inner nuclear membrane. The ER-GCaMP6-150 probe allowed us to directly visualize a third pool of mGlu₅ receptors, namely those located on the ER, an organelle difficult to isolate in a functionally intact state. Similar to mGlu₅ activity in purified striatal nuclei, the activation of ER-restricted mGlu₅ produced faster, larger, and longer effects visualized with the ER-GCaMP6-150 probe than did the activation of the cell surface receptor. At peak response times, cell surface responses were ~64% of the mGlu₅ ER response in cell bodies and 53% in neurites (Figure 3C–E). In keeping with ER peak responses being larger, the amount of Ca²⁺ released was much greater, being ~2-fold more within the cell body and ~4-fold more in neurites, measuring the area of the Ca²⁺ curve from initiation outwards to 100 s (n = 12 neurons/each condition) [20,22]. ER-restricted, mGlu₅-mediated Ca²⁺ responses were blocked by the Gq inhibitor, FR9000359, the PLC inhibitor, U73122, as well as both IP₃ and ryanodine receptor blockers. Thus, activated ER-restricted mGlu₅ receptors signal via the same canonical G_{q/11}/PLC/IP₃ pathway that is found at the plasma membrane as well as the inner nuclear membrane [34–40]. Taken together, these data reinforce the notion that mGlu₅ can signal from different membrane platforms to generate downstream sequelae with unique spatiotemporal profiles.

Although DHPG has been widely used to simulate a specific mGlu₅ receptor response (e.g., “chemical” LTD in hippocampal slices) [41], it is glutamate that is released at the synapse and is transported into the cell where, as we have shown, it can activate the large intracellular pool of mGlu₅ receptors [19]. In striatal, cortical, and spinal cord dorsal horn neurons, we have found that DHPG activation of cell surface mGlu₅ elicited a rapid, transient Ca²⁺ response, whereas Quis (or glutamate) activation of intracellular mGlu₅ produced sustained Ca²⁺ responses [18,20,21]. Not surprisingly, these unique spatiotemporal differences led to markedly different signaling outcomes. For example, we found that intracellular mGlu₅ primarily uses protein synthesis-dependent MEK/ERK pathways to generate striatal LTD, whereas cell surface mGlu₅ uses mammalian target of rapamycin complex 2 (mTORC2) [22]. Thus, it is critical to recognize that glutamate is not just activating its plethora of ionotropic and metabotropic receptors on the cell surface but, at least for mGlu₅ and mGlu₁, it is activating intracellular components as well.

Although generally considered to be a continuous organelle, within neurons, the ER itself is highly compartmentalized, ranging from tubules and cisternae in dendrites to sheetlike cisternae in the soma and then very narrow tubules running down the axons [42]. As the major intracellular Ca²⁺ reservoir, ER regulation of Ca²⁺ signaling is highly involved in many functions including neurotransmitter release at synapses, protein synthesis, folding, and transport throughout the neuron, especially in somatodendritic regions. ER Ca²⁺ signaling is also responsible for integrating cellular interactions with other organelles like the mitochondria and plasma membranes to maintain homeostasis [43–45].

Many processes have been implicated in the ER release of Ca²⁺ store regulation including Ca²⁺ entry via NMDA receptors which, in turn, can trigger ryanodine receptor activation and further ER Ca²⁺ release [29–33]. Activation of NMDA receptors in striatal cultures did not release Ca²⁺ from the ER (Figure 5B,C), nor did we find any evidence of ER fission in striatal neurons in which several groups have reported to be associated with

NMDA-mediated ER Ca^{2+} release [33]. It has also been reported that AMPAR-associated Ca^{2+} influx might contribute to this process. Given that we included an AMPA receptor inhibitor in the culture media prior to mGlu₅ agonist treatments, it seems doubtful that either ionic glutamate receptor is playing a role in this paradigm. Moreover, in the past, we have directly tested for AMPAR agonist effects in both wild-type and mGlu₅ KO cultures and have seen no change in baseline Ca^{2+} levels using cytoplasmic Ca^{2+} fluorophores [18]. As an additional control in those experiments, we also tested the NMDA inhibitor, APV, and saw no effect either [18]. Thus, we concluded that neither NMDARs nor AMPARs are contributing to the release of Ca^{2+} from the ER in our dissociated striatal culture paradigm.

Taken together, all of our data are consistent with activation of intracellular mGlu₅ directly releasing ER Ca^{2+} . Collectively, these data underscore the importance of intracellular mGlu₅ in the cascade of events underlying sustained synaptic transmission.

5. Conclusions

Although past experiments have used caged ligand and real-time imaging to show that intracellular mGlu₅ is functional in dendrites, as the largest intracellular organelle, the ER extends throughout the cell, forming a complex network of tubules and sheets. Since it is impossible to isolate the entire organelle, the newly developed Ca^{2+} indicator, ER-GCaMP6-150, allows for the study of ER-localized mGlu₅ function in situ. Using this tool, we found that activation of ER-localized mGlu₅ resulted in pronounced somal Ca^{2+} declines compared to the cell surface receptor. Akin to the cell surface receptor, decreases in luminal Ca^{2+} were coupled to $G_{q/11}$ and PLC to generate IP₃-mediated release of Ca^{2+} from Ca^{2+} release channels in the ER. ER-localized mGlu₅ effects were twice as large and more rapid than those triggered by cell surface mGlu₅, especially in striatal neurites. Thus, the ER can function as an autonomous organelle mobilizing Ca^{2+} in a specific, localized fashion.

Author Contributions: Y.-J.I.J. and K.L.O. designed the study and wrote the paper. S.K.H. prepared the primary cultures. Y.-J.I.J. carried out the experiments and analyzed the data. All authors have read and agreed to the published version of the manuscript.

Funding: This work was supported, in whole or in part, by National Institutes of Health Grants MH119197 (to K.L.O.), NS102783 (to K.L.O.), MH101874 (to K. L.O), and IDDRC Grant P50 HD103525. Confocal data were generated on an Olympus Confocal Microscope through the use of Washington University Center for Cellular Imaging (WUCCI) supported by the Washington University School of Medicine, The Children's Discovery Institute of Washington University and St. Louis Children's Hospital (CDI-CORE-2015-505 and CDI-CORE-2019-813), the Bantley Foundation, and the Foundation for Barnes-Jewish Hospital (3770 and 4642). The content is solely the responsibility of the authors and does not necessarily represent the official views of the National Institutes of Health.

Institutional Review Board Statement: All animal procedures were performed according to NIH guidelines and approved by the Washington University Institutional Animal Care and Use Committee under protocol 24-0024 approved on 9 February 2024.

Informed Consent Statement: Not applicable.

Data Availability Statement: Data used in this study are located in the article or are available upon request.

Conflicts of Interest: The authors declare no other competing financial interests.

References

1. Berridge, M.; Lipp, P.; Bootman, M. Calcium signalling. *Curr. Biol.* **1999**, *9*, R157–R159. [[CrossRef](#)]
2. Berridge, M.J.; Bootman, M.D.; Roderick, H.L. Calcium signalling: Dynamics, homeostasis and remodelling. *Nat. Rev. Mol. Cell Biol.* **2003**, *4*, 517–529. [[CrossRef](#)] [[PubMed](#)]

3. Bootman, M.D.; Bultynck, G. Fundamentals of Cellular Calcium Signaling: A Primer. *Cold Spring Harb. Perspect. Biol.* **2019**, *12*, a038802. [\[CrossRef\]](#) [\[PubMed\]](#)
4. Kilpatrick, L.E.; Hill, S. Transactivation of G protein-coupled receptors (GPCRs) and receptor tyrosine kinases (RTKs): Recent insights using luminescence and fluorescence technologies. *Curr. Opin. Endocr. Metab. Res.* **2021**, *16*, 102–112. [\[CrossRef\]](#) [\[PubMed\]](#)
5. Mikoshiba, K. The InsP3 receptor and intracellular Ca₂₊ signaling. *Curr. Opin. Neurobiol.* **1997**, *7*, 339–345. [\[CrossRef\]](#)
6. Foskett, J.K.; White, C.; Cheung, K.H.; Mak, D.O. Inositol trisphosphate receptor Ca₂₊ release channels. *Physiol. Rev.* **2007**, *87*, 593–658. [\[CrossRef\]](#)
7. Berridge, M.J. The inositol trisphosphate/calcium signaling pathway in health and disease. *Physiol. Rev.* **2016**, *96*, 1261–1296. [\[CrossRef\]](#)
8. Carreras-Sureda, A.; Pihán, P.; Hetz, C. Calcium signaling at the endoplasmic reticulum: Fine-tuning stress responses. *Cell Calcium* **2018**, *70*, 24–31. [\[CrossRef\]](#)
9. Hermans, E.; Challiss, R.J. Structural, signalling and regulatory properties of the group I metabotropic glutamate receptors: Prototypic family C G-protein-coupled receptors. *Biochem. J.* **2001**, *359*, 465–484. [\[CrossRef\]](#)
10. Moldrich, R.X.; Beart, P.M. Emerging signalling and protein interactions mediated via metabotropic glutamate receptors. *Curr. Drug Target.-CNS Neurol. Disord.* **2003**, *2*, 109–122. [\[CrossRef\]](#)
11. Flint, A.C.; Dammerman, R.S.; Kriegstein, A.R. Endogenous activation of metabotropic glutamate receptors in neocortical development causes neuronal calcium oscillations. *Proc. Natl. Acad. Sci. USA* **1999**, *96*, 12144–12149. [\[CrossRef\]](#) [\[PubMed\]](#)
12. Kettunen, P.; Krieger, P.; Hess, P.D.; El Manira, A. Signaling mechanisms of metabotropic glutamate receptor 5 subtype and its endogenous role in a locomotor network. *J. Neurosci.* **2002**, *22*, 1868–1873. [\[CrossRef\]](#) [\[PubMed\]](#)
13. Marino, M.; Awad-Granko, H.; Ciombor, K.; Conn, P. Haloperidol-induced alteration in the physiological actions of group I mGlu in the subthalamic nucleus and the substantia nigra pars reticulata. *Neuropharmacology* **2002**, *43*, 147–159. [\[CrossRef\]](#) [\[PubMed\]](#)
14. Jong, Y.-J.I.; Harmon, S.K.; O'malley, K.L. Intracellular GPCRs Play Key Roles in Synaptic Plasticity. *ACS Chem. Neurosci.* **2018**, *9*, 2162–2172. [\[CrossRef\]](#)
15. Jong, Y.I.; Harmon, S.K.; O'Malley, K.L. GPCR signalling from within the cell. *Br. J. Pharmacol.* **2018**, *175*, 4026–4035. [\[CrossRef\]](#)
16. Jong, Y.I.; Harmon, S.K.; O'Malley, K.L. GPCR Signaling from Intracellular Membranes. In *GPCRs as Therapeutic Targets Chapter 8*; Gilchrist, A., Ed.; Wiley: Hoboken, NJ, USA, 2022. [\[CrossRef\]](#)
17. Jong, Y.-J.I.; Kumar, V.; Kingston, A.E.; Romano, C.; O'Malley, K.L. Functional metabotropic glutamate receptors on nuclei from brain and primary cultured striatal neurons. Role of transporters in delivering ligand. *J. Biol. Chem.* **2005**, *280*, 30469–30480. [\[CrossRef\]](#)
18. Jong, Y.-J.I.; Kumar, V.; O'Malley, K.L. Intracellular metabotropic glutamate receptor 5 (mGluR5) activates signaling cascades distinct from cell surface counterparts. *J. Biol. Chem.* **2009**, *284*, 35827–35838. [\[CrossRef\]](#)
19. Purgert, C.A.; Izumi, Y.; Jong, Y.-J.I.; Kumar, V.; Zorumski, C.F.; O'Malley, K.L. Intracellular mGluR5 can mediate synaptic plasticity in the hippocampus. *J. Neurosci.* **2014**, *34*, 4589–4598. [\[CrossRef\]](#)
20. Vincent, K.; Cornea, V.M.; Jong, Y.-J.I.; Laferrière, A.; Kumar, N.; Mickeviciute, A.; Fung, J.S.T.; Bandegi, P.; Ribeiro-Da-Silva, A.; O'malley, K.L.; et al. Intracellular mGluR5 plays a critical role in neuropathic pain. *Nat. Commun.* **2016**, *7*, 10604. [\[CrossRef\]](#)
21. Jong, Y.I.; Harmon, S.K.; O'Malley, K.L. Location and Cell-Type-Specific Bias of Metabotropic Glutamate Receptor, mGlu5, Negative Allosteric Modulators. *ACS Chem. Neurosci.* **2019**, *10*, 4558–4570. [\[CrossRef\]](#)
22. Jong, Y.-J.I.; Izumi, Y.; Harmon, S.K.; Zorumski, C.F.; O'malley, K.L. Striatal mGlu5-mediated synaptic plasticity is independently regulated by location-specific receptor pools and divergent signaling pathways. *J. Biol. Chem.* **2023**, *299*, 104949. [\[CrossRef\]](#) [\[PubMed\]](#)
23. Kumar, V.; Jong, Y.J.; O'Malley, K.L. Activated nuclear metabotropic glutamate receptor mGlu5 couples to nuclear Gq/11 proteins to generate inositol 1,4,5-trisphosphate-mediated nuclear Ca₂₊ release. *J. Biol. Chem.* **2008**, *283*, 14072–14083. [\[CrossRef\]](#) [\[PubMed\]](#)
24. de Juan-Sanz, J.; Holt, G.T.; Schreiter, E.R.; de Juan, F.; Kim, D.S.; Ryan, T.A. Axonal Endoplasmic Reticulum Ca₂₊ Content Controls Release Probability in CNS Nerve Terminals. *Neuron* **2017**, *93*, 867–881. [\[CrossRef\]](#)
25. Onken, M.D.; Makepeace, C.M.; Kaltenbronn, K.M.; Kanai, S.M.; Todd, T.D.; Wang, S.; Broekelmann, T.J.; Rao, P.K.; Cooper, J.A.; Blumer, K.J. Targeting nucleotide exchange to inhibit constitutively active G protein α subunits in cancer cells. *Sci. Signal.* **2018**, *11*, eaao6852. [\[CrossRef\]](#)
26. Mao, L.; Wang, J.Q. Upregulation of preprodynorphin and preproenkephalin mRNA expression by selective activation of group I metabotropic glutamate receptors in characterized primary cultures of rat striatal neurons. *Mol. Brain Res.* **2001**, *86*, 125–137. [\[CrossRef\]](#)
27. Zhu, T.; Gobeil, F.; Vazquez-Tello, A.; Leduc, M.; Rihakova, L.; Bossolasco, M.; Bkaily, G.; Peri, K.; Varma, D.R.; Orvoine, R.; et al. Intracrine signaling through lipid mediators and their cognate nuclear G-protein-coupled receptors: A paradigm based on PGE₂, PAF, and LPA1 receptors. *Can. J. Physiol. Pharmacol.* **2006**, *84*, 377–391. [\[CrossRef\]](#)

28. O'Malley, K.L.; Jong, Y.-J.I.; Gonchar, Y.; Burkhalter, A.; Romano, C. Activation of metabotropic glutamate receptor mGlu5 on nuclear membranes mediates intranuclear Ca_{2+} changes in heterologous cell types and neurons. *J. Biol. Chem.* **2003**, *278*, 28210–28219. [[CrossRef](#)]
29. Hardingham, G.E.; Arnold, F.J.L.; Bading, H. Nuclear calcium signaling controls CREB-mediated gene expression triggered by synaptic activity. *Nat. Neurosci.* **2001**, *4*, 261–267. [[CrossRef](#)]
30. Carrasco, M.A.; Jaimovich, E.; Kemmerling, U.; Hidalgo, C. Signal transduction and gene expression regulated by calcium release from internal stores in excitable cells. *Biol. Res.* **2004**, *37*, 701–712. [[CrossRef](#)]
31. Goussakov, I.; Miller, M.B.; Stutzmann, G.E. NMDA-mediated $\text{Ca}(2+)$ influx drives aberrant ryanodine receptor activation in dendrites of young Alzheimer's disease mice. *J. Neurosci.* **2010**, *30*, 12128–12137. [[CrossRef](#)]
32. Zieminska, E.; Stafiej, A.; Toczyłowska, B.; Albrecht, J.; Lazarewicz, J.W. Role of Ryanodine and NMDA Receptors in Tetrabromobisphenol A-Induced Calcium Imbalance and Cytotoxicity in Primary Cultures of Rat Cerebellar Granule Cells. *Neurotox. Res.* **2015**, *28*, 195–208. [[CrossRef](#)] [[PubMed](#)]
33. Kucharz, K.; Krogh, M.; Na Ng, A.; Toresson, H. NMDA receptor stimulation induces reversible fission of the neuronal endoplasmic reticulum. *PLoS ONE* **2009**, *4*, e5250. [[CrossRef](#)] [[PubMed](#)]
34. Buchner, K.; Otto, H.; Hilbert, R.; Lindschau, C.; Haller, H.; Hucho, F. Properties of protein kinase C associated with nuclear membranes. *Biochem. J.* **1992**, *286*, 369–375. [[CrossRef](#)] [[PubMed](#)]
35. Humbert, J.-P.; Matter, N.; Artault, J.-C.; Köppler, P.; Malviya, A.N. Inositol 1,4,5-trisphosphate receptor is located to the inner nuclear membrane vindicating regulation of nuclear calcium signaling by inositol 1,4,5-trisphosphate. Discrete distribution of inositol phosphate receptors to inner and outer nuclear membranes. *J. Biol. Chem.* **1996**, *271*, 478–485. [[CrossRef](#)]
36. Irvine, R. Nuclear lipid signaling. *Sci. STKE* **2000**, *48*, re1. [[CrossRef](#)]
37. Divecha, N.; Clarke, J.H.; Roefs, M.; Halstead, J.R.; D'santos, C. Nuclear inositides: Inconsistent consistencies. *Cell. Mol. Life Sci.* **2000**, *57*, 379–393. [[CrossRef](#)]
38. D'Santos, C.; Clarke, J.H.; Roefs, M.; Halstead, J.R.; Divecha, N. Nuclear inositides. *Eur. J. Histochem.* **2000**, *44*, 51–60.
39. Willard, F.S.; Crouch, M.F. Nuclear and cytoskeletal translocation and localization of heterotrimeric G-proteins. *Immunol. Cell Biol.* **2000**, *78*, 387–394. [[CrossRef](#)]
40. Gerasimenko, J.V.; Maruyama, Y.; Yano, K.; Dolman, N.J.; Tepikin, A.V.; Petersen, O.H.; Gerasimenko, O.V. NAADP mobilizes Ca_{2+} from a thapsigargin-sensitive store in the nuclear envelope by activating ryanodine receptors. *J. Cell Biol.* **2003**, *163*, 271–282. [[CrossRef](#)]
41. Huber, K.M.; Roder, J.C.; Bear, M.F. Chemical Induction of mGluR5- and Protein Synthesis-Dependent Long-Term Depression in Hippocampal Area CA1. *J. Neurophysiol.* **2001**, *86*, 321–325. [[CrossRef](#)]
42. Schwarz, D.S.; Blower, M.D. The endoplasmic reticulum: Structure, function and response to cellular signaling. *Cell Mol. Life Sci.* **2016**, *73*, 79–94. [[CrossRef](#)] [[PubMed](#)]
43. Parkkinen, I.; Their, A.; Asghar, M.Y.; Sree, S.; Jokitalo, E.; Airavaara, M. Pharmacological Regulation of Endoplasmic Reticulum Structure and Calcium Dynamics: Importance for Neurodegenerative Diseases. *Pharmacol. Rev.* **2023**, *75*, 959–978. [[CrossRef](#)] [[PubMed](#)]
44. Zheng, S.; Wang, X.; Zhao, D.; Liu, H.; Hu, Y. Calcium homeostasis and cancer: Insights from endoplasmic reticulum-centered organelle communications. *Trends Cell Biol.* **2023**, *33*, 312. [[CrossRef](#)]
45. Karagas, N.E.; Venkatachalam, K. Roles for the Endoplasmic Reticulum in Regulation of Neuronal Calcium Homeostasis. *Cells* **2019**, *8*, 1232. [[CrossRef](#)]

Disclaimer/Publisher's Note: The statements, opinions and data contained in all publications are solely those of the individual author(s) and contributor(s) and not of MDPI and/or the editor(s). MDPI and/or the editor(s) disclaim responsibility for any injury to people or property resulting from any ideas, methods, instructions or products referred to in the content.